

# 1 Thermomechanical testing under operating conditions of A516Gr70 2 used for CSP storage tanks 3

4 Cristina Prieto<sup>1</sup>, Camila Barreneche<sup>2</sup>, Mònica Martínez<sup>2</sup>, Luisa F. Cabeza<sup>3</sup>, A. Inés Fernández<sup>2,\*</sup>  
5

6 <sup>1</sup>Abengoa Research, C/ Energía Solar nº 1, Palmas Altas,41014-Sevilla

7 <sup>2</sup> Department of Materials Science & Physical Chemistry, Universitat de Barcelona, Martí i Franqués 1,  
8 Barcelona 08028, Spain.

9 <sup>3</sup> GREA Innovació Concurrent, INSPIRES Research Centre, Universitat de Lleida, Pere de Cabrera s/n,  
10 25001, Lleida, Spain.

11 \*Corresponding authors: ana\_inesfernandez@ub.edu

## 12 Abstract

13 Thermal energy storage (TES) in molten salts is the storage dominating technology in solar  
14 power applications today. In two-tank molten salt storage systems energy density ranges from  
15 30 to 70 kWh/m<sup>3</sup> are achievable. The salt material used is a binary system, composed of 60%  
16 NaNO<sub>3</sub> and 40% KNO<sub>3</sub>. In the 8 MWh<sub>th</sub> pilot plant built and tested by Abengoa, the storage  
17 tanks were made of steel A516Gr.70 using the Appendix M of code API 650 for their design. A  
18 specific testing device was developed to evaluate thermo-mechanical properties, and a study  
19 was conducted in order to evaluate tensile properties of A516Gr.70 specimens under operation  
20 conditions for the hot tank at the pilot plant that is in contact with molten salts at 380 °C.  
21 Results confirmed the outcomes of the work: the reduction of the yield limit, elongation before  
22 fracture, and Young modulus at 380 °C after having been 5 minutes immersed in molten salts.  
23 Moreover, after a creep-test simulating operating 7 days conditions during, an additional  
24 reduction of the yield limit was measured.

25  
26 Key-words: *thermomechanical properties, concentrated solar power (CSP), thermal energy*  
27 *storage (TES), carbon steel, molten salts, thermal treatment*

## 28 1. Introduction

29 The global crisis of energy is one of the biggest challenges for the near future for researchers  
30 and policy makers in order to achieve a sustainable solution that deal with this energy crisis [1-  
31 2]. Solar energy is the highest power source of the world. Thereby, solar power technologies are  
32 able to produce high amounts of sustainable power. Concentrated solar power (CSP) plants [3-  
33 4] are systems able to concentrate a large amount of solar energy using different types of  
34 collectors; several characteristics of solar power plants are described by Desideri et al. [5].

35 Nowadays, thermal energy storage (TES) is a promising technology to be applied as a  
36 complement of CPS plants in order to reduce the gap between energy supply and energy  
37 demand [6]. Therefore, TES systems are implemented in CSP plants successfully by producing  
38 electricity several hours after sunrise [7]. Moreover, TES will help in making CSP much more  
39 viable and feasible from the economic and technical point of view. But the proper selection of  
40 materials has a great significance not only to deal with a proper performance of the plant but  
41 also for the economic interest of TES units.

42 A516Gr.70 steel was used to manufacture the storage tanks in the pilot plant of nitrate molten  
43 salts with 8 MWh<sub>th</sub> built by Abengoa [8]. A516Gr.70 is the main used steel in commercial CSP  
44 plants due to its high mechanical performance efficiency under stress and its relative low cost.  
45 Mechanical design typically uses the yield strength as one of the main design parameters.  
46 However, it is well known that the mechanical properties of steels as the yield strength or the  
47 modulus of elasticity decrease with increasing temperature. In this study, this change is of  
48 extremely importance because during operation of both storage tanks, the cold one is designed  
49 to operate at 288 °C and the hot one at 388 °C. Moreover, the maximum service temperature is  
50 the highest temperature at which the material can be used for an extended period without  
51 significant problems [9]. For the majority of commercial carbon steels, this temperature ranges  
52 from 270 to 360°C and only few grades of steel are certified to work at higher temperatures like  
53 the operation conditions of the hot tank of molten salts storage systems. Prieto et al. [8]  
54 previously reported a detailed description of the tanks design. Both tanks were built with steel  
55 A516 and two grades with different grain size. Thus, grade 60 with the smallest grain size was  
56 used for the tank cover and grade 70 for the rest of the tank. Parameters used for the design were  
57 those of the Appendix M of code API 650, although it only gives the requirements for working  
58 temperatures between 90 °C and 260 °C.

59 The study of the evolution of the mechanical properties with temperature may be performed  
60 varying temperature with special testing devices adapted for such purpose, and following  
61 international standards for testing [11]. Nevertheless, the working conditions of this material in  
62 operation, which are the temperature (388 °C) and the environment (in contact with nitrate  
63 molten salts), are not considered in any standard. For this purpose, a study was conducted in  
64 order to evaluate tensile properties under operation conditions by testing in a device developed  
65 at the University of Barcelona, where a series of mechanical experiments were performed with  
66 A516 gr70 carbon steel specimens in contact with molten salts at 380 °C. Prior and after the  
67 mechanical testing, a metallographic study was performed.

68

69 **2. Methods and materials**

70 **2.1. Materials**

71 The specimens for this study were obtained from a plate of the same carbon steel used in the  
 72 construction of the tanks at the Abengoa plant. Table 1 summarizes the main characteristics  
 73 collected from the CES Selector database for the reference ASTM A516 Grade 70 Carbon Steel  
 74 Plate for Boilers and Pressure Vessels.

75

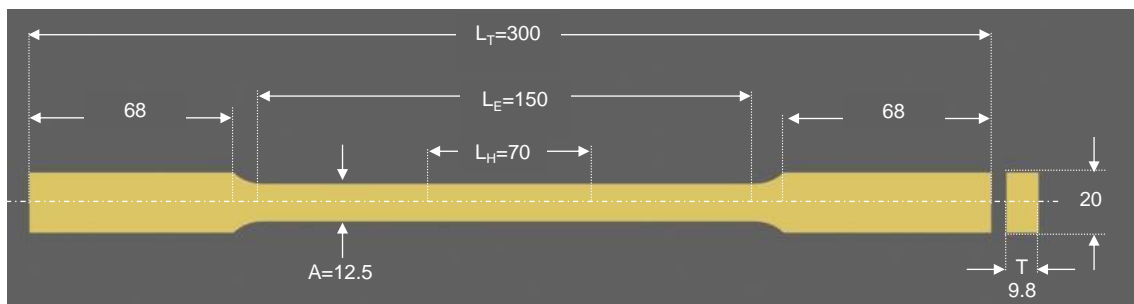
76 **Table 1. Composition of Carbon steel A516 Grade 70 [12].**

Composition	Content (% wt.)
Fe (Iron)	Base Element (>98)
C (Carbon)	0.27
Mn (Manganese)	0.79-1.3
S (Sulphur)	0.025
Si (Silicon)	0.025
<b>Mechanical properties</b>	
Ultimate tensile strength (UTS)	485 – 620 MPa
Yield Strength	260 MPa (minimum value)
Elongation	15% (minimum value)

77

78 Specimens for mechanical testing were machined from the original plate by laser cutting. The  
 79 size of the specimens was calculated following the standard from the plate thickness [11].  
 80 Dimensions (in millimetres) and design of the specimens are shown in Figure 1.

81



82

83 **Figure 1 - Dimensions of the specimens machined from A516Gr70 plate [11].**

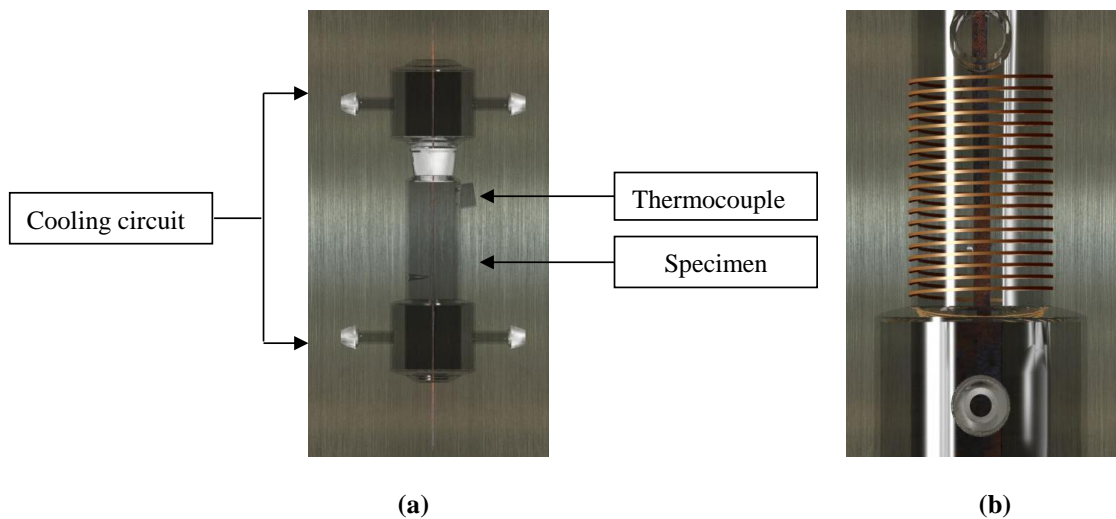
84

85           **2.2. Experimental set up**

86    A small furnace was designed and built at University of Barcelona to perform the tests at the  
87    desired temperature (in this case 380 °C), having the specimen in contact with nitrate molten  
88    salts during the mechanical testing. The mixture selected is the so-called *Solar salt* reported in  
89    the literature with a composition 60:40 NaNO<sub>3</sub> and KNO<sub>3</sub> by weight, close to the eutectic  
90    composition.

91    The cylindrical device was made of quartz, and its size allows testing the central part of the  
92    samples. A specific opening was designed to introduce a thermocouple to monitor the molten  
93    salts temperature as shows the scheme of Figure 2.(a). The top and the bottom of the device are  
94    designed so that a refrigeration circuit using water as heat transfer fluid may be coupled, to  
95    prevent molten salts leakage. Furthermore, it also has the central part with a reduced section in  
96    which an electrical resistance was coiled around, see Figure 2.(b), and then fully thermally  
97    insulated, see Figure 3.

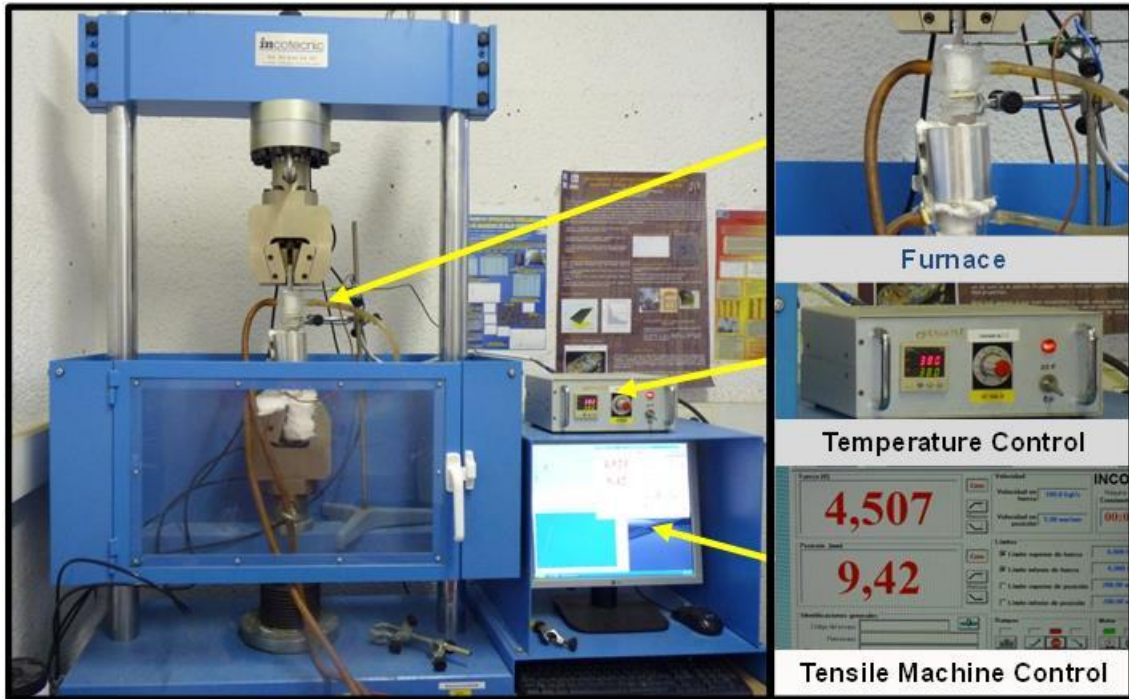
98



99           **Figure 2. (a) Small furnace devise; (b) Heating source**

100    The insulated system keeping the length of reduced section of the specimen in contact with  
101    molten salts is presented in the upper right part of Figure 3. The sample is then fixed through the  
102    jaws to the mechanical testing machine Incotecnic MUTC-200.

103



104

105

**Figure 3 - Picture of the experimental set-up**

106

107 In order to evaluate the effect of temperature on the mechanical behaviour, three different  
 108 experiments were performed.

109 First experiment: the material under study was first tested at room temperature. The tensile test  
 110 was carried out at a loading rate of  $5 \text{ mm} \cdot \text{min}^{-1}$  until failure. Then, the conventional diagrams  
 111 plotting stress ( $\sigma$ ) vs. % strain ( $\epsilon\%$ ), where stress and strain are defined with Eq. 1 and Eq. 2,  
 112 were calculated:

113

$$\sigma \text{ (MPa)} = \frac{F \text{ (N)}}{S \text{ (mm}^2\text{)}} \quad \text{Eq. 1}$$

$$\% \epsilon = \frac{\Delta l \text{ (mm)}}{l \text{ (mm)}} \times 100 \quad \text{Eq. 2}$$

114

115 where  $F$  is the applied force (in  $N$ ) and  $S$  is the area perpendicular to the application of force, in  
 116 the case of the specimens tested it is  $122.5 \text{ mm}^2$  and to calculate it,  $l$  is fixed to  $205 \text{ mm}$ , being  
 117 the distance between jaws.

118 The yield strength obtained from the conventional diagram was used as a reference yield  
 119 strength to perform the next mechanical tests at higher temperature.

120 Second experiment: the effect of the temperature on the mechanical properties was tested using  
121 the device described previously, having the central part with reduced section in contact with the  
122 molten salts at 380 °C. Notice that the sample was in contact with the molten salts not only  
123 during the mechanical-test but also during the heating processes (the heating rate applied was 5  
124 °C·min<sup>-1</sup>). Once the temperature of the salts reached 380 °C, the sample was left five more  
125 minutes to homogenize the temperature of the specimen. Afterwards, the specimen was tested at  
126 380 °C under a loading rate of 5 mm·min<sup>-1</sup> until the sample fractured in order to observe if the  
127 temperature affected the mechanical properties. It is important to remark that the main objective  
128 of performing these tensile strength tests (out of standards) is to determine the temperature  
129 effect instead of determining high precision values for mechanical properties. Even though, the  
130 obtained results can be used to perform a comparison in order to differentiate mechanical  
131 behaviours, being this comparison semi-quantitative.

132 Third experiment: as seen so far, the mechanical behaviour of the steel tested change when  
133 working at high temperature. In order to determine a possible variation of the properties under  
134 working conditions (load, temperature, and contact with molten salts) a specific experiment was  
135 designed. It consists in applying a load (39200 N) and keeping the specimen contact with  
136 molten salts during 7 days under a constant elongation (4.79 mm): this test is known as creep-  
137 test in materials engineering field.

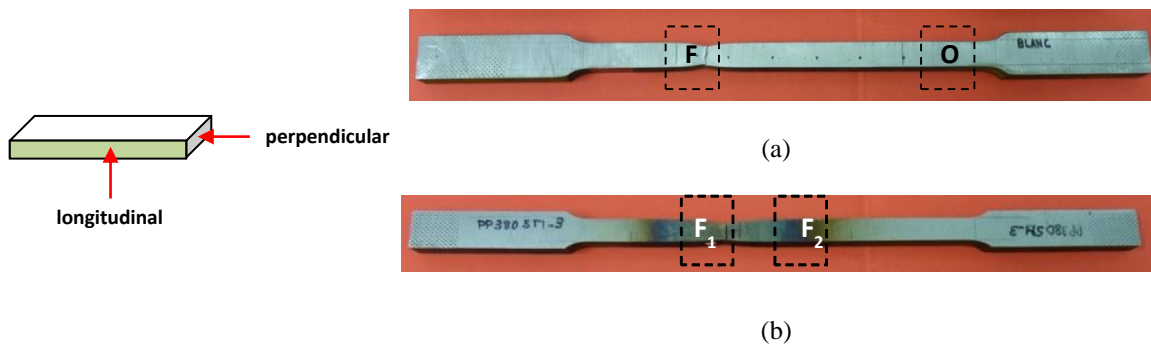
138 The experimental procedure consisted on applying an initial load. This load has to be below the  
139 one obtained by measuring yield strength of a A516Gr70 steel sample immersed in molten salts  
140 at 380 °C (second experiment).. Therefore, regarding the load a safety factor of 1.25 was used to  
141 perform thermo-mechanical experiments, which is commonly used for exceptionally reliable  
142 materials used under controllable conditions [9]. After the creep-test, a tensile strength test was  
143 performed at 380 °C (inside the device) under a loading rate of 5 mm·min<sup>-1</sup> until the sample  
144 fracture too.

145

### 146 **2.3. Metallographic study**

147 After the failure, different zones of the tested specimen at 380 °C were cut and prepared for the  
148 metallographic study. Sample preparation follows the ASTM standard [13] for steel samples,  
149 and the etching agent used to reveal the microstructure was Nital (98%v/v ethanol, 2%v/v  
150 HNO<sub>3</sub>).

151 For each sample, the microstructure was observed in two different zones: zone F is the failure  
152 zone and zone O is a zone of the reduced section far from the failure. Moreover, the  
153 microstructure was observed from both applied force directions, longitudinal and perpendicular  
154 to the application of stress as Figure 4 shows.



156 **Figure 4 - Zones where the metallographic study was performed with (a) samples measured under**  
 157 **380 °C and (b) sample tested under 380 °C after 7 days**

158 Notice that the temperature of F, F1 and F2 zones were at 380 °C because these zones are inside  
 159 the furnace and 25 °C is the temperature outside the furnace (O zone).

160

### 161 3. Results and discussion

#### 162 3.1. Mechanical testing

163 Mechanical properties obtained from the tensile strength test under room temperature conditions  
 164 are shown in Figure 5 (blue line). The yield strength obtained ( $\sigma_{0.2}$ ) is ~400 MPa and the  
 165 elongation 17%. Comparing these results with the specifications for a steel of this grade, the  
 166 yield obtained in the test performed is well above the minimum specified for this material (260  
 167 MPa), while the measured elongation is slightly higher than the minimum specified (15%). In  
 168 addition, tensile strength test results for the sample tested at 380 °C in contact during 5 minutes  
 169 with molten salts are also shown in Figure 5 (orange line). In this case, the yield strength ( $\sigma_{0.2}$ )  
 170 is about 340 MPa and the strain percentage 13%, showing lower plastic deformation. To  
 171 calculate the strain the initial length used was  $L_0 = 205$  mm in order to use the same one than in  
 172 the test before (ambient temperature). In this test, the reduction of the Young Modulus with  
 173 temperature is also noticeable. The change of this and other properties is described following  
 174 the equation [14]:

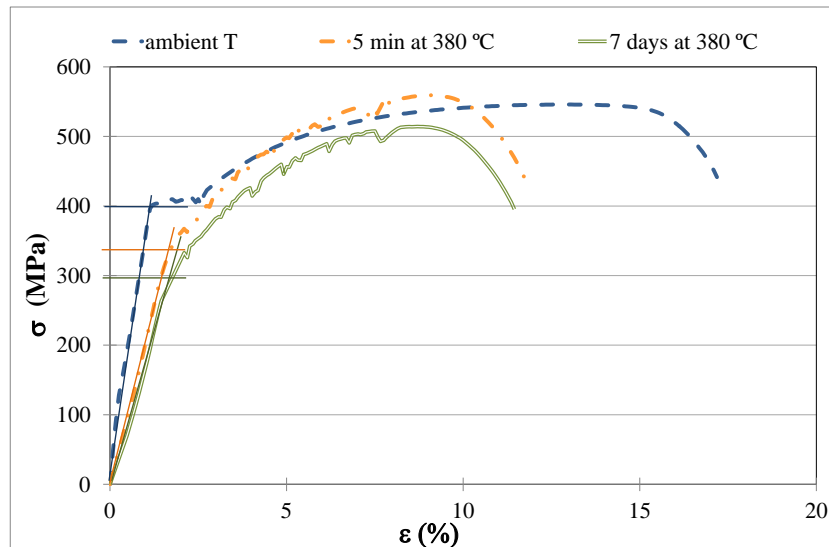
175

$$176 \quad P \approx P_0 \left( 1 + \beta \frac{T}{T_m} \right) \quad \text{Eq. 3}$$

177

178 where  $P$  is the property at a given temperature  $T$  (K),  $P_0$  is the property at 25°C,  $\beta$  is a constant  
 179 ( $\beta \approx -0.5$  for metals), and  $T_m$  is the melting temperature (K). This equation predicts a reduction

180 of the Young Modulus of around 19% that should be also considered during the mechanical  
181 design. But in the experiments presented, 40% reduction of Young Modulus was calculated  
182 from the obtained curves. A more accurate Young Modulus values could be expected with the  
183 use of an extensometer, but this device is not available.



184

185 **Figure 5 - Conventional diagram of A516GR70 specimen tested at room temperature (blue line),**  
186 **tested at 380 °C (orange line), and tested at 380 °C after 7 days creep-test (green line)**

187

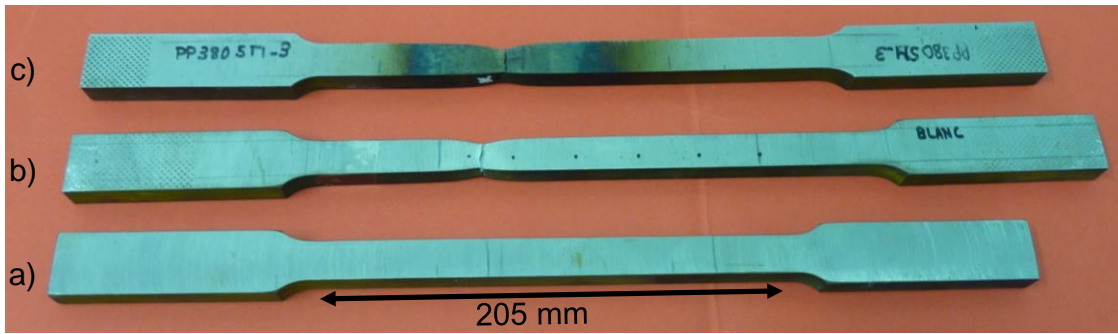
188 The part of the specimen in contact with the molten salts at 380 °C begins to deform plastically  
189 at a lower load, while the rest of the specimen is at a lower temperature, still working in the  
190 elastic range. This assumption is verified by measuring the dimensions of the specimens after  
191 the test.

192 In the sample tested at 380 °C, dimensions change only in the region in contact with molten  
193 salts, whereas in the specimen tested at room temperature, all the central part with a reduced  
194 section changed its dimensions.

195 In the sample tested at room temperature (blue line), when the stress is increased, the strain is  
196 slightly increased (steep slope) until a critical stress value (yield strength). After that, low  
197 increments in load produced high elongation (yield zone). The behaviour shown in this area is  
198 due to oblique surface slides caused by shear stress (Luders bands). However, when the  
199 material is tested under 380 °C, the yield zone disappears because the temperature disables  
200 sliding surface mechanisms [15] or the temperature decreases the yield strength.

201 Finally, Figure 6 shows the specimens that have undergone necking in the area of rupture,  
202 showing a ductile failure with plastic deformation in both cases (room temperature and under  
203 380 °C).

204



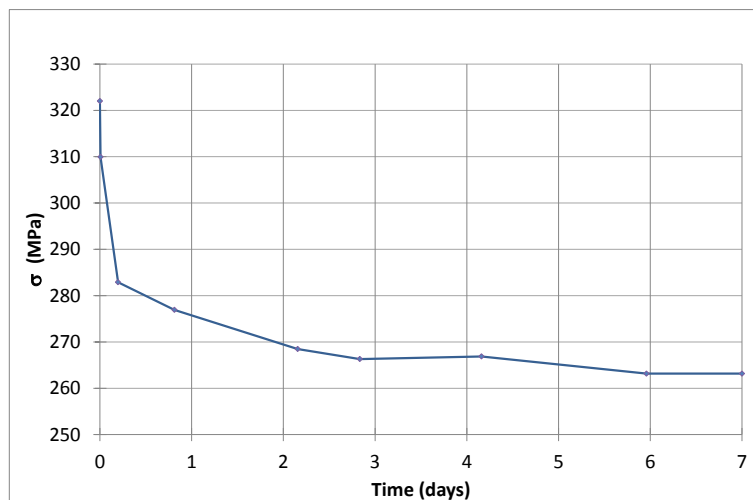
205

206 **Figure 6 - Specimen of A516GR70 (a) before the tensile strength test, (b) after the tensile test at**  
207 **room temperature, (c) after the tensile test at 380 °C**

208

209 In order to evaluate the performance under operational conditions, the sample was tested at 380  
210 °C in contact with molten salts during 7 days by applying an initial load of 320 MPa (below the  
211 yield strength measured at 380 °C). The elongation produced by applying this load was 4.79  
212 mm. Then, this elongation was kept constant during the 7 days of test and load was registered  
213 over time. Notice that the stress required to keep a constant elongation decreases over time to an  
214 asymptotic value (approximately 265 MPa) due to stress relaxation, as Figure 7 shows.

215



216

217 **Figure 7 - Change in the stress needed to keep a constant elongation of 4.79 mm at 380 °C**

218

219 Once 7 days have elapsed, a new tensile test was performed on the sample and the conventional  
220 diagram obtained is also shown in Figure 5. Thereby, the yield strength is less than 300 MPa,  
221 about 40 MPa lower than that obtained when the specimen had only been 5 minutes at 380 °C  
222 (Figure 6). The elongation at fracture was very similar while the measured yield strength was

223 higher than the 260 MPa accepted as minimum value in the standard. The material anneals from  
224 the beginning and this annealing continues during this period of 7 days of performance under  
225 load, at 380 °C and in contact with molten salts.

226 Therefore, when a creep test is performed (7 days, 380 °C, 320 MPa) the sample is plastically  
227 deformed, and hence, in a posterior tensile strength test the deformation mechanisms are  
228 disabled due to the previous plastic deformation [14] and the ultimate tensile strength also  
229 decreased.

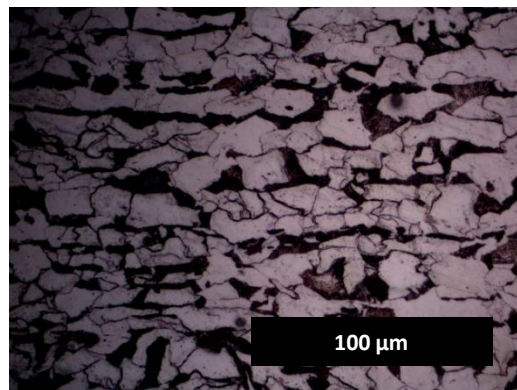
230

### 231 3.2. Metallographic study

232 Since there were differences in the mechanical response upon the testing conditions, the study  
233 of the microstructure prior and after each step was done to complement the obtained results.

234 The longitudinal section of the initial microstructure at 50x magnification is shown in Figure 8.  
235 The grains are equiaxially oriented following the shaping direction of the sheet.

236



237

238 **Figure 8- Initial longitudinal microstructure of A516Gr70 carbon steel sample**

239

240 The microstructure of samples tested at room temperature is shown in Figure 9 applying 50x  
241 magnification. Figure 9.(a) and 9.(b) show a microstructure with oriented equiaxial grains, due  
242 to the shaping of the sheet. In the image of the longitudinal failure zone shown in Figure 10.(c),  
243 the grains deformed in the direction of application of force during the tensile test are observed.  
244 Moreover, notice that the grains became smaller due to the force applied, as Figure 9.(d) shows.

245 On the other hand, Figure 9.(e) and Figure 9.(f) show the areas where the microstructure and the  
246 longitudinal and cross direction of samples tested at 380 °C during 7 days can be seen. The  
247 longitudinal failure zone ( $F_1$ ) observed in Figure 9.(e) shows that the grains are deformed in the  
248 direction of the applied force ( $\uparrow$ ). Moreover, the cross-section of the broken zone ( $F_1$ ) is shown

249 in Figure 9.(f) where the grains are highly deformed losing their initial form. On the other hand,  
250 the grains are slightly affected and preserve almost the same form as the original one in the  
251 longitudinal section outside of the failure zone ( $F_2$ ), as shown in Figure 9.(g).

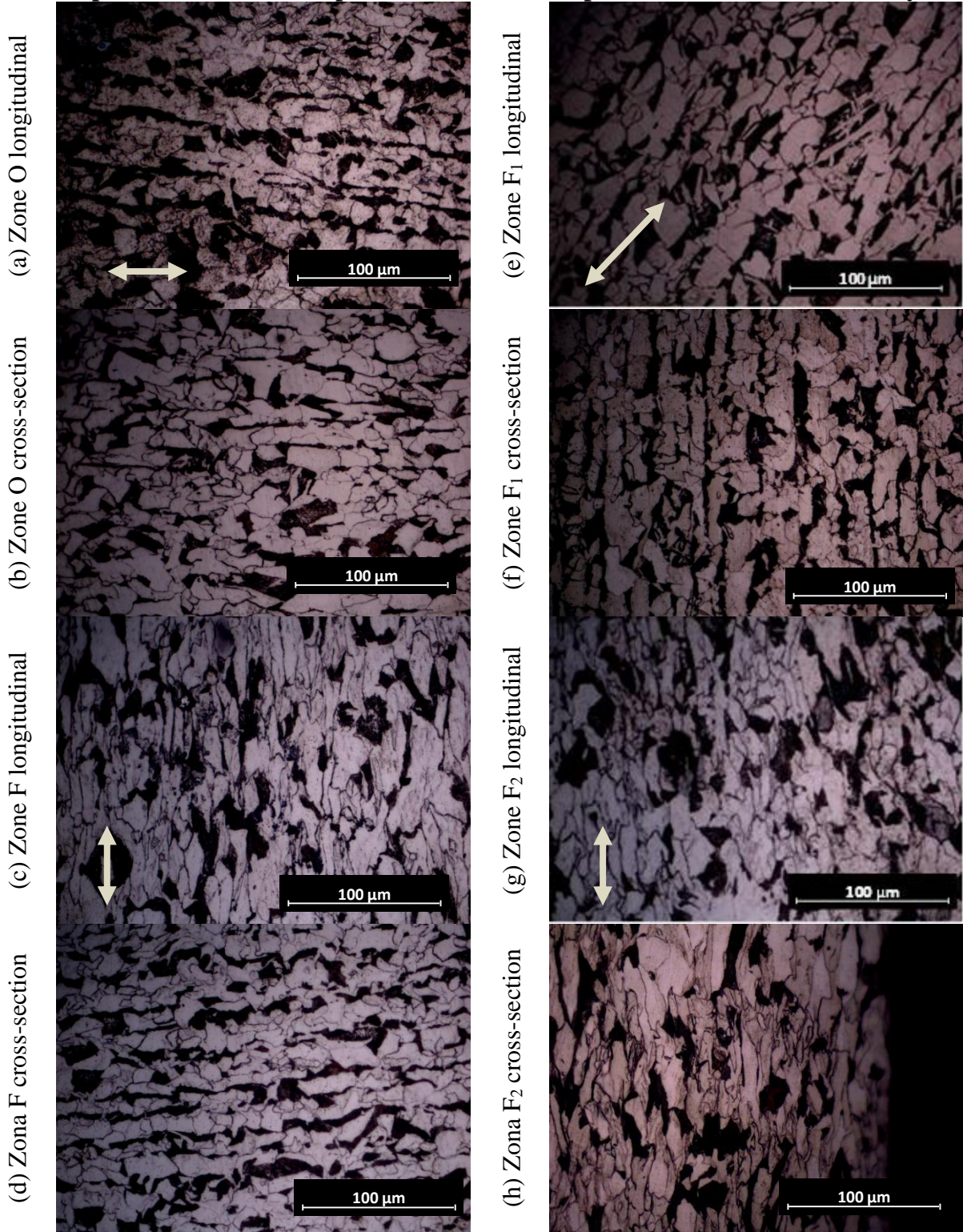
252 Even though the operational conditions are reported as corrosives, corrosion evidences appear at  
253 longer exposure times and there is no evidence of intergranular corrosion in the metallographic  
254 analysis of samples under load at 380 °C, in contact with molten salts for 7 days.

255 The reduction of yield strength and elongation is attributed to the annealing of the sample and  
256 this fact is corroborated with the metallographic study as shown in the deformation in  
257 concordance with the direction (see Figure 9).

258

**Sample tested at room temperature**

**Sample tested at 380 °C after 7 days**



259 Figure 9- Microstructure of the samples tested under the following conditions: (a) Longitudinal section outside  
 260 of the broken part of the samples tested at room temperature; (b) Cross-section outside of the broken part of  
 261 the samples tested at room temperature; (c) Longitudinal section outside of the broken part of the samples  
 262 tested at room temperature; (d) Cross-section outside of the broken part of the samples tested at room  
 263 temperature; (e) Longitudinal section in the broken part of the samples treated at 380 °C during 7 days; (f)  
 264 Cross-section in the broken part of the samples treated at 380 °C during 7 days; (g) Longitudinal section  
 265 outside of the broken part of the samples treated at 380 °C during 7 days; (h) Cross-section section outside of  
 266 the broken part of the samples treated at 380 °C during 7 days

267 \* Notice that arrows indicate the direction load applied during the tensile strength test

#### 268 **4. Conclusions**

269 An experimental setup to perform the mechanical testing of steel A516Gr70 under operational  
270 conditions at 380 °C in contact with molten salts was designed and built.

271 Mechanical testing under operational conditions confirmed the reduction of yield strength and  
272 Young Modulus as well as the elongation compared with testing at room temperature. The  
273 measured yield strength is above the limit defined in the ASTM standard.

274 A seven days creep-test experiment maintaining the sample under working conditions and a  
275 load below the yield strength was performed. Changes in mechanical properties after the creep-  
276 test are confirmed: the reduction of yield strength and elongation are attributed to the annealing  
277 of the sample and this fact is corroborated with the metallographic study carried out.

#### 278 279 **Acknowledgements**

280 The research leading to these results has received funding from Spanish government (Fondo  
281 tecnológico IDI-20090393, ConSOLida CENIT 2008-1005). The work is partially funded by the  
282 Spanish government (ENE2011-28269-C03-02, ENE2011-22722, ENE2015-64117-C5-1-R,  
283 and ENE2015-64117-C5-2-R). The research leading to these results has received funding from  
284 the European Union's Seventh Framework Programme (FP7/2007-2013) under grant agreement  
285 n° PIRSES-GA-2013-610692 (INNOSTORAGE) and from the European Union's Horizon 2020  
286 research and innovation programme under grant agreement No 657466 (INPATH-TES). The  
287 authors would like to thank the Catalan Government for the quality accreditation given to their  
288 research groups GREA (2014 SGR 123) and research group DIOPMA (2014 SGR 1543). Dr.  
289 Camila Barreneche would like to thank Ministerio de Economía y Competitividad de España for  
290 Grant Juan de la Cierva FJCI-2014-22886.

#### 291 292 **References**

- 293
- 294 1. V. Devabhaktuni, M. Alam, Shekara Sreenadh Reddy Depuru, S. Green II, R.C. Nims,  
295 D., C. Near. Solar energy trends and enabling technologies. *Renew Sustain Energy Rev*,  
296 19 (2013), pp. 555–564.
  - 297  
298 2. Chu Y. Review and comparison of different solar energy technologies. *Research*  
299 *Associate Global Energy Network Institute (GENI)*, vol. 619; 2011, p. 595-0139.
- 300

- 301 3. U.S. Department of Energy. Integrated solar thermochemical reaction system. Available  
302 from: [http://energy.gov/eere/sunshot/project-profile-integrated-solar-thermochemical-  
304 reaction-system](http://energy.gov/eere/sunshot/project-profile-integrated-solar-thermochemical-<br/>303 reaction-system) (retrieved 01.12.2016)
- 304 4. Jibrán Khan, Mudassar H. ArsalanSolar power technologies for sustainable electricity  
305 generation – A review. *Renewable and Sustainable Energy Reviews* 55 (2016) 414–  
306 425.
- 307 5. U. Desideri, F. Zepparelli, V. Morettini, E. Garroni. Comparative analysis of  
308 concentrating solar power and photovoltaic technologies: technical and environmental  
309 evaluations. *Appl Energy*, 102 (2013), pp. 765–784
- 310 6. Ming Liu, Wasim Saman, Frank Bruno. Review on storage materials and thermal  
311 performance enhancement techniques for high temperature phase change thermal  
312 storage Systems. *Renewable and Sustainable Energy Reviews* 16 (2012) 2118–2132
- 313 7. Sarada Kuravi, Jamie Trahan, D. Yogi Goswami, Muhammad M. Rahman, Elias K.  
314 Stefanakos. Thermal energy storage technologies and systems for concentrating solar  
315 power plants. *Progress in Energy and Combustion Science* Volume 39, Issue 4, August  
316 2013, Pages 285–319
- 317 8. Prieto C, Fernández AI, Cabeza LF. Molten salt facilities, lessons learnt at pilot plant  
318 scale to guarantee commercial plants. Plant description and start-up recommendations.  
319 Accepted for publication in *Renewable Energy*
- 320 9. Ugural, A. C. Mechanical design. An integrated approach. Mac Graw Hill, 2004 (p52)  
321 USA. ISBN 0-07-242155-X
- 322 10. Prieto C; Fernández, A.I.; Cabeza, L.F. Molten salt facilities, lessons learnt at pilot plant  
323 scale to guarantee commercial plants. Part 1 – Plant description and start-up  
324 recommendations (paper submitted to *Renewable Energy*).
- 325 11. ASTM Standard: ASTM E8 / E8M - 15a. Standard Test Methods for Tension Testing of  
326 Metallic Materials
- 327 12. CES Selector Database. Granda Design, Cambridge 2012.
- 328 13. ASM International. ASM Handbook: Metallografy and microstructures, vol 9. UK.  
329 ISBN: 0-87170-706-3. 2004.
- 330 14. Ashby MF, Shercliff H, Cebon D. *Materials: Engineering, Science, Processing and  
331 Design*. Butterworth-Heinemann, 2007, ISBN 9870750683913.
- 332 15. Beer FP, Russell Johnston Jr. E, DeWolf JT, Mazurek DF. *Mechanics of materials*. Mc  
333 Graw Hill, 7<sup>th</sup> edition, 2015, 978-0073398235.